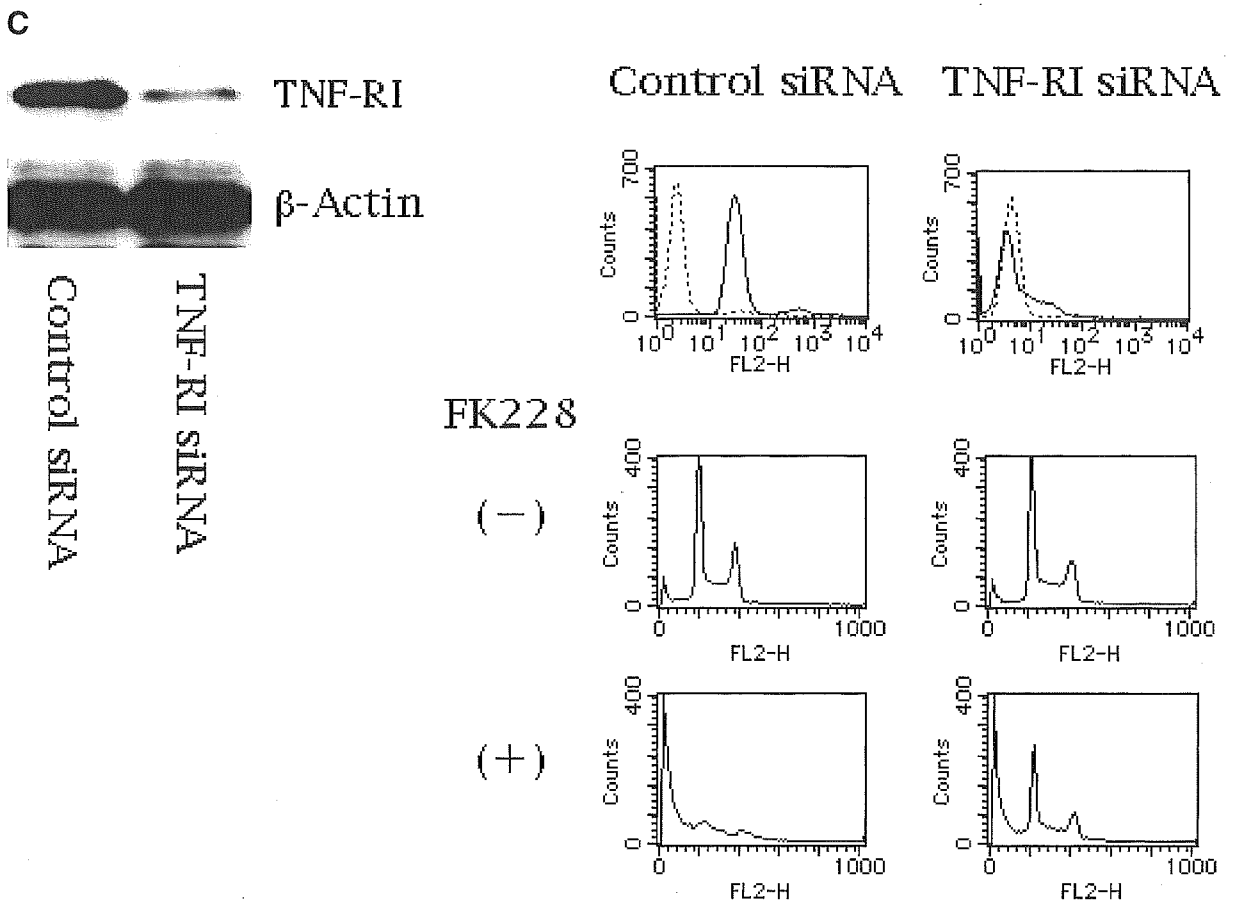

Fig. 4. (*Continued*)

TNF-α gene through hyperacetylation of histones H3 and H4 of its promoter regions. It has been shown that transcription of the TNF-α gene is governed by the formation of stimuli-specific enhancer complexes containing histone acetyltransferases CBP/p300 (Barthel et al., 2003). Depsipeptide (FK228) bypasses the requirement of the enhancer complexes, and aberrantly induces transcription of the TNF-α gene in myeloid leukemia cells. This information is not only useful for cancer treatment, but also applicable to pharmacological interventions for other inflammatory and immunological processes associated with activation of TNF-α.

In summary, the present study has defined autocrine production of TNF-α as an important mediator of the cytotoxic effects of depsipeptide (FK228) in a subset of myeloid leukemias. It is assumed, however, that many

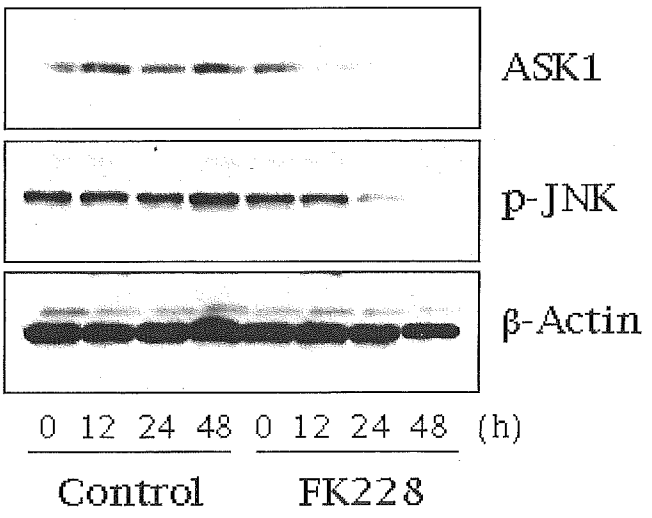

Fig. 5. Effects of depsipeptide (FK228) on the Jun kinase cascade. Whole cell lysates were prepared from HL-60 cells at the indicated time points, and subjected to immunoblot analysis for the expression of ASK1, phosphorylated JNK, and β-actin. The data shown are representative of two independent experiments.

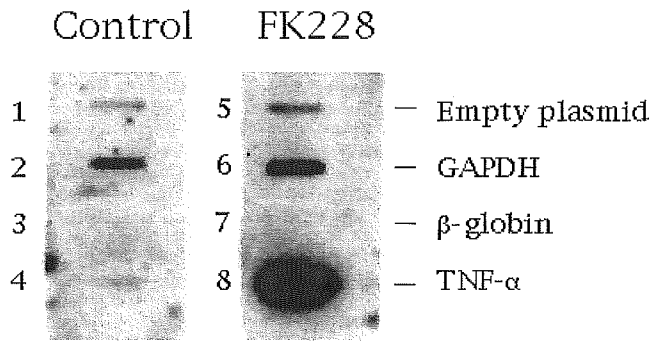

Fig. 6. Nuclear run-on assay for TNF-α transcription in depsipeptide-treated HL-60 cells. Nascent nuclear RNA was elongated in the presence of [^{32}P]UTP in HL-60 cells cultured with (control) or without 20 nM depsipeptide (FK228) for 6 h, and hybridized to immobilized plasmids containing cDNAs for GAPDH (lanes 2 and 6), β-globin (lanes 3 and 7), and TNF-α (lanes 4 and 8) on nylon membranes. Empty pCRII vector was used as a negative control (lanes 1 and 5). The data shown are representative of multiple independent experiments.

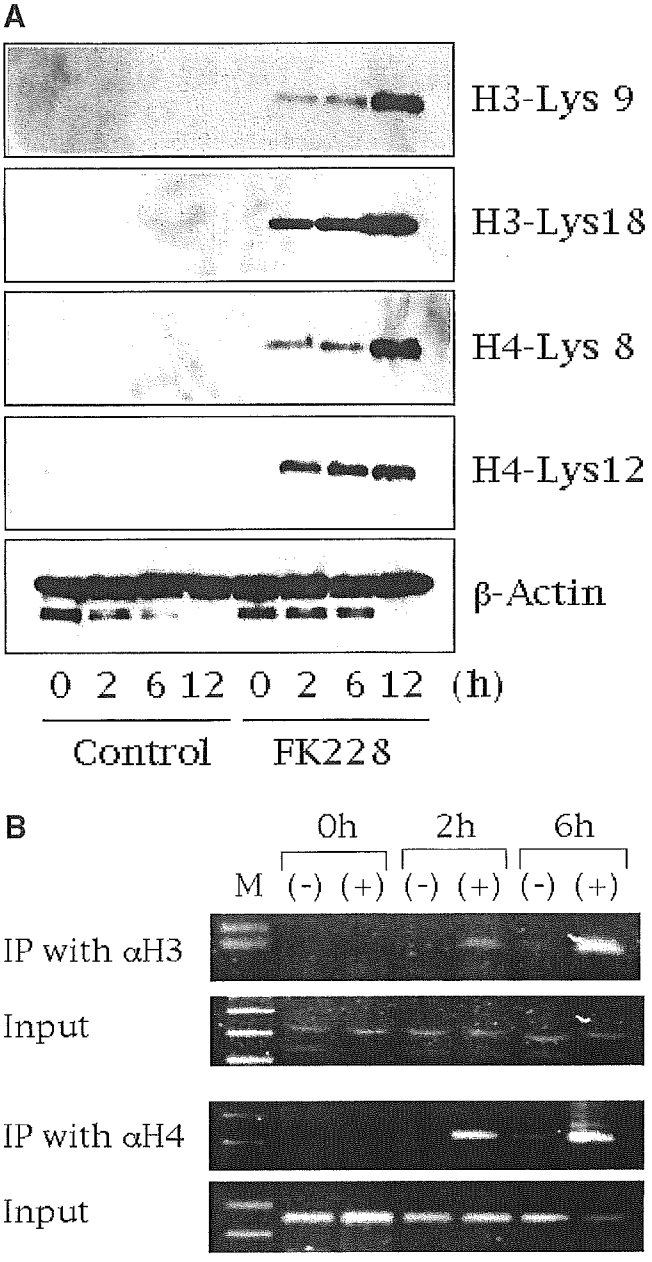

Fig. 7. Depsipeptide-induced hyperacetylation of TNF-α promoter in HL-60 cells. **A**: Acetylation of histone tails in depsipeptide-treated HL-60 cells. Whole cell lysates were prepared as described in Figure 3, and subjected to immunoblotting with the site-specific anti-acetylated histone antibodies indicated on the right. The membrane filters were reprobed with anti-β-actin antibody to verify the equal loading and integrity of samples. **B**: ChIP assay for acetylation of TNF-α promoter. After crosslinking with formaldehyde, chromatin suspensions were prepared from HL-60 cells treated with (+) or without (−) depsipeptide for 0, 2, and 6 h, and subjected to immunoprecipitation with antibodies against acetylated histones H3 and H4. The resulting precipitants were subjected to PCR using a specific primer pair corresponding to nucleotide positions −208 to +35 of the TNF-α promoter. PCR was carried out for 30 cycles, and the amplified products were visualized by ethidium bromide staining after 2% agarose gel electrophoresis. Input: Prior to the immunoprecipitation, 1/40 of the sonicated cell suspension was saved and used for PCR after reversal of the crosslinking. The data shown are representative of multiple independent experiments.

factors are involved in the pharmacological actions of depsipeptide (FK228). Our study will provide a clue as to further elucidate the molecular basis of the action of this potential drug for refractory leukemias.

ACKNOWLEDGMENTS

The study is supported in part by grants-in-aid for scientific research from the Ministry of Education, Science and Culture of Japan, and by the Japan Leukemia Research Fund.

LITERATURE CITED

Agalioti T, Chen G, Thanos D. 2002. Deciphering the transcriptional histone acetylation code for a human gene. Cell 111:381–392.

Amin HM, Saeed S, Alkan S. 2001. Histone deacetylase inhibitors induce caspase-dependent apoptosis and downregulation of daxx in acute promyelocytic leukaemia with t(15;17). Br J Haematol 115:287–297.

Aron JL, Parthun MR, Marcucci G, Kitada S, Mone AP, Davis ME, Shen T, Murphy T, Wickham J, Kanakry C, Lucas DM, Reed JC, Grever MR, Byrd JC. 2003. Depsipeptide (FR901228) induces histone acetylation and inhibition of histone deacetylation in chronic lymphocytic leukemia cells concurrent with activation of caspase-8-mediated apoptosis and down-regulation of c-FLIP protein. Blood 102:652–658.

Baker SJ, Reddy EP. 1998. Modulation of life and death by the TNF receptor superfamily. Oncogene 17:3261–3270.

Baker PK, Pettitt AR, Slupsky JR, Chen HJ, Glenn MA, Zuzel M, Cawley JC. 2002. Response of hairy cells to IFN-α involves induction of apoptosis through autocrine TNF-α and protection by adhesion. Blood 100:647–653.

Barnhart BC, Peter ME. 2003. The TNF receptor 1: A split personality complex. Cell 114:148–150.

Barthel R, Tsytsykova AV, Barczak AK, Tsai EY, Dascher CC, Brenner MB, Goldfeld AE. 2003. Regulation of tumor necrosis factor alpha gene expression by mycobacteria involves the assembly of a unique enhanceosome dependent on the coactivator proteins CBP/p300. Mol Cell Biol 23:526–533.

Bernhard D, Ausserlechner MJ, Tonko M, Loffler M, Hartmann BL, Csordas A, Kofler R. 1999. Apoptosis induced by the histone deacetylase inhibitor sodium butyrate in human leukemic lymphoblasts. FASEB J 13:1991–2001.

Budihardjo I, Oliver H, Lutter M, Luo X, Wang X. 1999. Biochemical pathways of caspase activation during apoptosis. Annu Rev Cell Dev Biol 15:269–290.

Byrd JC, Shinn C, Ravi R, Willis CR, Waselenko JK, Flinn IW, Dawson NA, Grever MR. 1999. Depsipeptide (FR901228): A novel therapeutic agent with selective, in vitro activity against human B-cell chronic lymphocytic leukemia cells. Blood 94:1401–1408.

Darzynkiewicz Z, Carter SP, Old LJ. 1987. Effect of recombinant tumor necrosis factor on HL-60 cells: Cell-cycle specificity and synergism with actinomycin D. J Cell Physiol 130:328–335.

Derjuga A, Richard C, Crosato M, Wright PS, Chalifour L, Valdez J, Barraso A, Crissman HA, Nishioka W, Bradbury EM, Th'ng JPH. 2001. Expression of $p21^{Waf1/Cip1}$ and cyclin D1 is increased in butyrate-resistant HeLa cells. J Biol Chem 276:37815–37820.

Falvo JV, Uglialoro AM, Brinkman BMN, Merika M, Parekh BS, Tsai EY, King HC, Morielli AD, Peralta EG, Maniatis T, Thanos D, Goldfeld AE. 2000. Stimulus-specific assembly of enhancer complexes on the tumor necrosis factor alpha gene promoter. Mol Cell Biol 20:2239–2247.

Fuchs P, Strehl S, Dworzak M, Himmler A, Ambros PF. 1992. Structure of the human TNF receptor 1 (p60) gene (TNFR1) and localization to chromosome 12p13. Genomics 13:219–224.

Furukawa Y, DeCaprio JA, Freedman AS, Kanakura Y, Nakamura M, Ernst TJ, Livingston DM, Griffin JD. 1990. Expression and state of phosphorylation of the retinoblastoma susceptibility gene product in cycling and noncycling human hematopoietic cells. Proc Natl Acad Sci USA 87:2770–2774.

Furukawa Y, Nishimura N, Furukawa Y, Satoh M, Endo H, Iwase S, Yamada H, Matsuda M, Kano Y, Nakamura M. 2002. Apaf-1 is a mediator of E2F-1-induced apoptosis. J Biol Chem 277:39760–39768.

Glaser KB, Staver MJ, Waring JF, Stender J, Ulrich RG, Davidsen SK. 2003. Gene expression profiling of multiple histone deacetylase (HDAC) inhibitors: Defining a common set produced by HDAC inhibition in T24 and MDA carcinoma cell lines. Mol Cancer Ther 2:151–163.

Gore SD, Weng L-J, Figg WD, Zhai S, Donehower RC, Dover G, Grever MR, Griffin C, Grochow LB, Hawkins A, Burks K, Zabelena Y, Miller CB. 2002. Impact of prolonged infusions of the putative differentiating agent sodium phenylbutyrate on myelodysplastic syndromes and acute myeloid leukemia. Clin Cancer Res 8:963–970.

Henderson C, Mizzau M, Paroni G, Maestro R, Schneider C, Brancolini C. 2003. Role of caspases, Bid, and p53 in the apoptotic response triggered by histone deacetylase inhibitors trichostatin-A (TSA) and suberoylanilide hydroxamic acid (SAHA). J Biol Chem 278:12579–12589.

Hong S-H, David G, Wong C-W, Dejean A, Privalsky ML. 1997. SMRT corepressor interacts with PLZF and with the PML-retinoic acid receptor α (RARα) and PLZF-RARα oncoproteins associated with acute promyelocytic leukemia. Proc Natl Acad Sci USA 94:9028–9033.

Jenuwein T, Allis CD. 2001. Translating the histone code. Science 293:1074–1080.

Johnstone RW, Licht JD. 2003. Histone deacetylase inhibitors in cancer therapy: Is transcription the primary target? Cancer Cell 4:13–18.

Khochbin S, Verdel A, Lemercier C, Seigneurin-Berny D. 2001. Functional significance of histone deacetylase diversity. Curr Opin Genet Dev 11:162–166.

Kim MS, Kwon HJ, Lee YM, Baek JH, Jang J-E, Lee S-W, Moon E-J, Kim H-S, Lee S-K, Chung HY, Kim CW. 2001. Histone deacetylases induce angiogenesis by negative regulation of tumor suppressor genes. Nature Med 7:437–443.

Kumakura S, Ishikura H, Maniwa Y, Munemasa S, Tsumura H, Masuda J, Kobayashi S. 2003. Activation of protein kinase C enhances TNF-alpha-induced differentiation by preventing apoptosis via rapid up-regulation of c-Myc protein expression in HL-60 cells. Leuk Lymphoma 44:497–503.

Kwon SH, Ahn SH, Kim YK, Bae G-U, Yoon JW, Hong S, Lee HY, Lee Y-W, Lee H-W, Han JW. 2002. Apicidin, a histone deacetylase inhibitor, induces apoptosis and Fas/Fas ligand expression in human acute promyelocytic leukemia cells. J Biol Chem 277:2073–2080.

Lin RJ, Nagy L, Inoue S, Shao W, Miller JWH, Evans RM. 1998. Role of the histone deacetylase complex in acute promyelocytic leukemia. Nature 391: 811–814.

Maeda T, Towatari M, Kosugi H, Saito H. 2000. Up-regulation of costimulatory/adhesion molecules by histone deacetylase inhibitors in acute myeloid leukemia cells. Blood 96:3847–3856.

Mariadason JM, Corner GA, Augenlicht LH. 2000. Genetic reprogramming in pathways of colonic cell mutation induced by short chain fatty acids: Comparison with trichostatin A, sulindac, and curcumin and implications for chemoprevention of colon cancer. Cancer Res 60:4561–4572.

Melnick A, Licht JD. 2002. Histone deacetylases as therapeutic targets in hematologic malignancies. Curr Opin Hematol 9:322–332.

Minucci S, Nervi C, Coco FL, Pelicci PG. 2001. Histone deacetylases: A common molecular target for differentiation treatment of acute myeloid leukemias? Oncogene 20:3110–3115.

Murata M, Towatari M, Kosugi H, Tanimoto M, Ueda R, Saito H, Naoe T. 2000. Apoptotic cytotoxic effects of a histone deacetylase inhibitor, FK228, on malignant lymphoid cells. Jpn J Cancer Res 91:1154–1160.

Nakayama J-I, Rice JC, Strahl BD, Allis CD, Grewal SIS. 2001. Role of histone H3 lysine 9 methylation in epigenetic control of heterochromatin assembly. Science 292:110–113.

Piekarz RL, Robey R, Sandor V, Bakke S, Wilson WH, Dahmoush L, Kingma DM, Turner ML, Altemus R, Bates SE. 2001. Inhibitor of histone deacetylation, depsipeptide (FR901228), in the treatment of peripheral and cutaneous T-cell lymphoma: A case report. Blood 98:2865–2868.

Qiu L, Burgess A, Fairlie DP, Leonard H, Parsons PG, Gabrielli BG. 2000. Histone deacetylase inhibitors trigger a G2 checkpoint in normal cells that is defective in tumor cells. Mol Biol Cell 11:2069–2083.

Richon VM, Sandhoff TW, Rifkind RA, Marks PA. 2000. Histond deacetylase inhibitor selectively induces $p21^{WAF1}$ expression and gene-associated histone deacetylation. Proc Natl Acad Sci USA 97:10014–10019.

Ruefli AA, Ausserlechner MJ, Bernhard D, Sutton VR, Tainton KM, Kofler R, Smyth MJ, Johnstone RW. 2001. The histone deacetylase inhibitor and chemotherapeutic agent suberoylanilide hydroxamic acid (SAHA) induces a cell-death pathway characetrized by cleavage of Bid and production of reactive oxygen species. Proc Natl Acad Sci USA 98:10833–10838.

Sandor V, Senderowicz A, Mertins S, Sackett D, Sausville E, Blagosklonny MV, Bates SE. 2000. P21-dependent G1 arrest with downregulation of cyclin D1 and upregulation of cyclin E by the histone deacetylase inhibitor FR901228. Br J Cancer 83:817–825.

Sandor V, Bakke S, Robery RW, Kang MH, Blagosklonny MV, Bender J, Brooks R, Piekarz RL, Tucker E, Figg WD, Chan KK, Goldspiel B, Fojo AT, Balcerzak SP, Bates SE. 2002. Phase I trial of the histone deacetylase inhibitor, depsipeptide (FR901228, NSC 630176), in patients with refractory neoplasms. Clin Cancer Res 8:718–728.

Suzuki H, Gabrielson E, Chen W, Anbazhagan R, van Engeland M, Weijenberg MP, Herman JG, Baylin SB. 2002. A genomic screen for genes upregulated by demethylation and histone deacetylase inhibition in human colorectal cancer. Nature Genet 31:141–149.

Taddei A, Maison C, Roche D, Almouzni G. 2001. Reversible disruption of pericentric heterochromatin and centromere function by inhibiting deacetylases. Nat Cell Biol 3:114–120.

Takashiba S, Shapira L, Amar S, Van Dyke TE. 1993. Cloning and characterization of human TNFα promoter region. Gene 131:307–308.

Ueda H, Manda T, Matsumoto S, Mukumoto S, Nishigaki F, Kawamura I, Shimomura K. 1994. FR901228, a novel antitumor bicyclic depsipeptide produced by *Chromobacterium violaceum* No. 968. J Antibiotic 47:315–323.

Wajant H, Johannes F-J, Haas E, Siemienski K, Schwenzer R, Schubert G, Weiss T, Grell M, Scheurich P. 1998. Dominant-negative FADD inhibits TNFR60-, Fas/Apo1- and TRAIL-R/Apo2-mediated cell death but not gene induction. Curr Biol 8:113–116.

Wang AM, Creasey AA, Ladner MB, Lin LS, Strickler J, Van Arsdell JN, Yamamoto R, Mark DF. 1985. Molecular cloning of the complementary DNA for human tumor necrosis factor. Science 228:149–154.

Wang J, Chun HJ, Wong W, Spencer DM, Lenardo MJ. 2001. Caspase-10 is an initiator caspase in death receptor signaling. Proc Natl Acad Sci USA 98: 13884–13888.

Warrell RPJ, He LZ, Richon V, Calleja E, Pandolfi PP. 1998. Therapeutic targeting of transcription in acute promyelocytic leukemia by use of an inhibitor of histone deacetylase. J Natl Cancer Inst 90:1621–1625.

Yamashita K, Upadhyay S, Osada M, Hoque MO, Xiao Y, Mori M, Sato F, Meltzer SJ, Sidransky D. 2002. Pharmacologic unmasking of epigenetically silenced tumor suppressor genes in esophageal squamous cell carcinoma. Cancer Cell 2:485–495.

Available online at www.sciencedirect.com
SCIENCE DIRECT
Biochemical Pharmacology 69 (2005) 1585–1594
Biochemical Pharmacology
www.elsevier.com/locate/biochempharm

Relative importance of apoptosis and cell cycle blockage in the synergistic effect of combined R115777 and imatinib treatment in BCR/ABL-positive cell lines

Takuji Miyoshi [a], Tadashi Nagai [a,*], Ken Ohmine [a], Makiko Nakamura [a], Yasuhiko Kano [b], Kazuo Muroi [c], Norio Komatsu [a], Keiya Ozawa [a]

[a] *Division of Hematology, Jichi Medical School, 3311-1 Yakushiji, Minamikawachi-machi, Kawachi-gun, Tochigi 329-0498, Japan*
[b] *Division of Hematology and Medical Oncology, Tochigi Cancer Center, Tochigi, Japan*
[c] *Cell Transplantation and Transfusion, Jichi Medical School, Tochigi, Japan*

Received 13 September 2004; accepted 9 February 2005

Abstract

The combination of imatinib and a farnesyltransferase inhibitor might be effective for reducing the number of BCR/ABL-positive leukemia cells. In this study, we examined the differences in the mechanisms of the growth inhibitory effect of the combination of imatinib and R115777 (Zarnestra^{TM}) among BCR/ABL-positive cell lines. Steel and Peckham isobologram analysis indicated that this combination had a strong synergistic inhibitory effect on growth in all imatinib-resistant cell lines and their parental cell lines. Levels of cleaved caspase 3 were increased by the combination treatment in all cell lines. However, both the level of cleaved PARP and the number of annexin-V-positive cells were much less increased in KCL22 and KCL22/SR cells than in K562, KU812, K562/SR and KU812/SR cells. The combination treatment promoted $p27^{KIP1}$ accumulation and induced a significant increase in the percentage of G0/G1 KCL22 and KCL22/SR cells. In other cell lines, the percentage of G0/G1 cells was not increased but rather decreased. The results indicate that induction of apoptosis and blockage of the cell cycle were major mechanisms of the synergistic inhibitory effect of the combination treatment, but the relative importance of these mechanisms differed among cell types. Additional treatment for overriding the G1 checkpoint may be required to eradicate leukemia cells, in which the combination induces cell cycle arrest.

Keywords: R115777; Farnesyltransferase inhibitor; Imatinib; BCR/ABL; Chronic myeloid leukemia; Drug resistance

1. Introduction

The ABL tyrosine kinase inhibitor imatinib mesylate (imatinib, Novartis) has shown a substantial clinical effect in BCR/ABL-positive leukemia patients [1–4]. It has been reported that about 50% of patients with aggressive BCR/ABL-positive leukemia, such as chronic myeloid leukemia in blast crisis (CML-BC) and acute lymphoblastic leukemia (ALL), exhibit a hematological response to treatment with imatinib alone [3,4]. However, most patients with such leukemia relapse soon after showing a response to imatinib; thus, long-term remission is not obtained with imatinib treatment alone. Furthermore, it is possible that many patients with CML-BC will have primary resistance to imatinib because imatinib may already have been administered in the chronic phase in many cases. Previous studies have demonstrated that BCR/ABL gene amplification, point mutations in the ATP-binding pocket of the BCR/ABL gene, increased expression of BCR/ABL protein, up-regulation of P-glycoprotein (P-gp) belonging to the ABC transporter family, increased concentration of serum α1 acid glycoprotein and up-regulation of Nrf2-mediated gene expressions may be involved in the acquisition of resistance to imatinib [5–14]. Several recent studies have indicated that imatinib-resistant cells with a point mutation in the BCR/ABL gene may be present prior to treatment with imatinib in BCR/ABL-positive leukemia patients [5,15–17]. Therefore, to obtain a sufficient clinical effect, it is important to reduce the number of imatinib-resistant leukemia cells by initial treatment targeting aggressive BCR/ABL-positive leukemia. Recently, a new generation of BCR/ABL kinase inhibitors has been developed [18–21] and has been shown to be effective

* Corresponding author. Tel.: +81 285 58 7353; fax: +81 285 44 5258.
E-mail address: t-nagai@jichi.ac.jp (T. Nagai).

0006-2952/$ – see front matter © 2005 Elsevier Inc. All rights reserved.
doi:10.1016/j.bcp.2005.02.021

against imatinib-resistant cells with point mutations in vitro [18]. However, none of these inhibitors are currently available for clinical use. At present, one attractive therapeutic strategy is combination therapy with imatinib and other anti-leukemia reagents. Cytotoxic effects of various combinations on leukemia cells have been investigated [22,23].

Some cellular proteins, including Ras family proteins, require posttranslational modifications to become active. Prenylation, which is involved in these modifications, can be performed by adding a 15-carbon farnesyl isoprenoid group mediated by farnesyltransferase. An alternative prenylation reaction, geranylgeranylation, can be performed by transferring a 20-carbon geranylgeranyl isoprenoid to proteins by geranylgeranyl transferases. Because prenylation is required to transfer Ras proteins to the cellular membrane, farnesyltransferase inhibitors (FTIs) were initially expected to suppress Ras function, leading to tumor growth inhibition [24,25]. An FTI showed significant anti-tumor activity via inhibition of H-Ras function in an activated H-Ras-induced breast cancer model [26]. However, N-Ras and K-Ras can be transferred to the cellular membrane by geranylgeranylation, even if farnesylation is inhibited, suggesting that inhibition of the processing of other target proteins is involved in the anti-tumor effects of FTIs. Such target proteins may include the small GTP-binding protein RhoB and the centromere-associated proteins CENP-E and CENP-F [27,28].

FTIs have been shown to have anti-leukemia effects on BCR/ABL-positive cultured cells and in BCR/ABL-positive murine models [29,30]. Moreover, Hoover et al. reported that an FTI, SCH66336, inhibited proliferation of imatinib-resistant cell lines and colony formation by hematopoietic progenitors from imatinib-resistant CML patients [31]. These findings suggest that FTIs have potential as agents for treatment of imatinib-resistant BCR/ABL-positive leukemia. The results of clinical studies on an FTI, R115777 (Zarnestra™, Titusville, NJ), indicate that it is moderately effective against CML [32,33]. However, R115777 alone does not seem to be sufficiently effective against aggressive CML [33]. Phase I studies using combination therapy with R115777 and imatinib for treatment of refractory or resistant BCR/ABL-positive leukemia have been conducted [34,35].

In this study, we investigated the mechanisms underlying the inhibitory effect of the combination of R115777 and imatinib on growth of BCR/ABL-positive cells. Our isobologram analysis revealed that this combination has a significant synergistic inhibitory effect on growth of imatinib-resistant cell lines and imatinib-sensitive cell lines. We also found that this effect was due to both induction of apoptosis and blockage of the cell cycle, but the relative importance of these two mechanisms differed among cell lines.

2. Materials and methods

2.1. Cell lines

We previously established an imatinib-resistant clone, KCL22/SR, from the KCL22 human BCR/ABL-positive cell line [36]. To obtain other imatinib-resistant clones, we treated K562 and KU812 cells (BCR/ABL-positive cell lines established from peripheral blood of CML patients in blast crisis) with step-wise increasing concentrations of imatinib (0.1–1.0 μM) and cultured them on a medium containing methylcellulose, followed by selection and cloning of individual colonies. These newly cloned imatinib-resistant cell lines were designated K562/SR and KU812/SR, respectively. All imatinib-sensitive parental cells and imatinib-resistant cells were grown in RPMI1640 medium supplemented with 10% fetal bovine serum and split every 4 days.

2.2. Cytotoxic effects of a combination of R115777 and imatinib

The farnesyltransferase inhibitor R115777 was kindly provided by Johnson & Johnson Pharmaceutical and Development (Philadelphia, PA). Imatinib was purchased from Novartis Pharma (Basel, Switzerland). Cells were incubated with various concentrations of each reagent for 4 days and then cell numbers were counted using a Cell Counting Kit-8 (Wako Pure Chemical Industries Ltd. Osaka, Japan) in accordance with the manufacturer's instructions. The cytotoxic effect of the combination of R115777 and imatinib was evaluated by a Steel and Peckham isobologram as described previously [37,38]. When the points were outside the left margin of the envelope formed by two broken lines, the combination treatment was considered to have a synergistic effect on cell growth inhibition. If the points were plotted within the envelope, the combination treatment was considered to have an additive effect.

2.3. Western blot analysis

Whole cell lysates were prepared from 1×10^7 cells according to a method described previously [39]. Then 10 μg of whole cell lysate was separated electrophoretically using 10% polyacrylamide gel. Immunoblotting and detection by enhanced chemiluminescence were performed as described previously [40]. Mouse anti-glyceraldehyde-3-phosphate dehydrogenase monoclonal antibody and anti-phospho-tyrosine antibody were purchased from Chemicon International (Temecula, CA) and Santa Cruz Biotechnology (Santa Cruz, CA), respectively. Anti-cleaved caspase 3, anti-PARP, anti-p44/42 (ERK1/2) MAP kinase and anti-phospho p44/42 (ERK1/2) MAP kinase rabbit polyclonal antibodies were purchased from Cell Signaling Technology (Beverly, MA). Mouse anti-

$p27^{KIP1}$ and anti-HDJ-2 monoclonal antibodies were purchased from BD Biosciences (San Jose, CA) and Neomarkers (Fremont, CA), respectively.

2.4. Flow cytometry

Apoptotic cells were evaluated by counting annexin-V-positive cells using a MEBCYTO-Apoptosis Kit (MBL, Nagoya, Japan) in accordance with the manufacturer's instructions. Briefly, the cells were collected and rinsed once with phosphate-buffered saline (PBS). The cells were then incubated with annexin-V-FITC and propidium iodide for 15 min and analyzed by flow cytometry using a FACScan Analyzer (Becton Dickinson, San Jose, CA). For cell cycle analysis, the cells were incubated with propidium iodide for 30 min and analyzed by flow cytometry using a FACScan/CellFIT system (Becton Dickinson, San Jose, CA).

3. Results

3.1. Development of imatinib-resistant BCR/ABL-positive cell lines

We used an imatinib-resistant clone, KCL22/SR, and its parental BCR/ABL-positive cell line, KCL22 [36]. In addition, we cloned two other imatinib-resistant clones, K562/SR and KU812/SR, from the BCR/ABL-positive cell lines K562 and KU812, respectively. As shown in Table 1, IC_{50} values of imatinib against the three imatinib-resistant clones were 5–9-fold higher than that against each corresponding parental cell line. No amplification of or point mutation in the BCR/ABL gene was found in these imatinib-resistant clones. Consistent with our previous findings [36], imatinib treatment resulted in a significant decrease in the level of phosphorylation of BCR/ABL protein in all imatinib-resistant clones as well as parental cell lines (data not shown). These results suggest that deregulation of processes downstream of BCR/ABL kinase is involved in the acquisition of resistance to imatinib in these imatinib-resistant clones.

3.2. Combined treatment of BCR/ABL-positive cells with R115777 and imatinib resulted in synergistic inhibition of cell growth

To confirm that the farnesyltransferase inhibitor R115777 inhibits farnesylation in BCR/ABL-positive cells, we examined the level of the chaperone protein HDJ-2, which is a substrate of farnesyltransferase, by Western blot analysis using an anti-HDJ-2 antibody [41]. Treatment of cells with R115777 resulted in significant accumulation of unprocessed HDJ-2 in all cell lines (data not shown), suggesting that farnesylation is effectively inhibited by R115777 in both imatinib-sensitive and imatinib-resistant BCR/ABL-positive cells. To determine whether a combination of R115777 and imatinib effectively inhibits growth of BCR/ABL-positive cells, we examined the time courses of changes in cell count after treatment with IC_{50} concentrations of imatinib, R115777 and a combination of these two reagents. The combined treatment resulted in greater suppression of cell growth than did treatment with either of the reagents alone in all parental and imatinib-resistant cells (data not shown). To determine whether the growth inhibitory effect was synergistic or additive, we next performed Steel and Peckham isobologram analysis, which provides very strict and reliable results [38]. Combined treatment of parental cells (KCL22, K562 and KU812) with R115777 and imatinib resulted in clear synergistic inhibition of cell growth (Fig. 1A). This combination also synergistically inhibited the growth of imatinib-resistant cells, KCL22/SR, K562/SR and KU812/SR (Fig. 1A). These results indicate that the combination of R115777 and imatinib has a synergistic inhibitory effect on growth of BCR/ABL-positive cells, regardless of sensitivity to imatinib.

R115777 was initially expected to be an inhibitor of Ras function. We investigated the levels of phosphorylation of ERK1/2, a Ras-mitogen-activated protein kinase (MAPK), to determine whether the synergistic inhibitory effect was mediated by alteration of Ras signaling. However, the levels of phopho-ERK1/2 were not decreased by R115777 treatment in any of the cell lines (data not shown). These results suggest that inhibition of Ras-MAPK signaling is not involved in the inhibitory effect of R115777 on BCR/ABL-positive cells.

Table 1
IC_{50} values of imatinib against the imatinib-sensitive and the imatinib-resistant cell lines

IC_{50} values(μM)		
KCL22 0.199 ± 0.037	KCL22/SR 1.779 ± 0.934	Ratio ×8.940
K562 0.218 ± 0.091	K562/SR 1.245 ± 0.419	Ratio ×5.711
KU812 0.216 ± 0.076	KU812/SR 1.526 ± 0.308	Ratio ×7.065

3.3. R115777 and imatinib synergistically inhibited the growth of leukemia cells from a patient in blast crisis

We next examined the effect of combined treatment on the growth of primary leukemia cells from a 53-year-old male patient in imatinib-resistant blast crisis. Written informed consent for the examination was obtained from the patient. Leukemia cells from peripheral blood of the patient, with no mutation in the BCR/ABL gene, were used for Steel and Peckham isobologram analysis. The patient showed no response to imatinib after conversion to blast crisis. The IC_{50} of imatinib to these cells was 0.71 μM, which is high compared with those of imatinib-sensitive CML cell lines. Combined treatment of these cells with R115777 and imatinib resulted in a synergistic inhibitory effect on growth (Fig. 1B). These results suggest that this combination treatment is effective against primary imati-

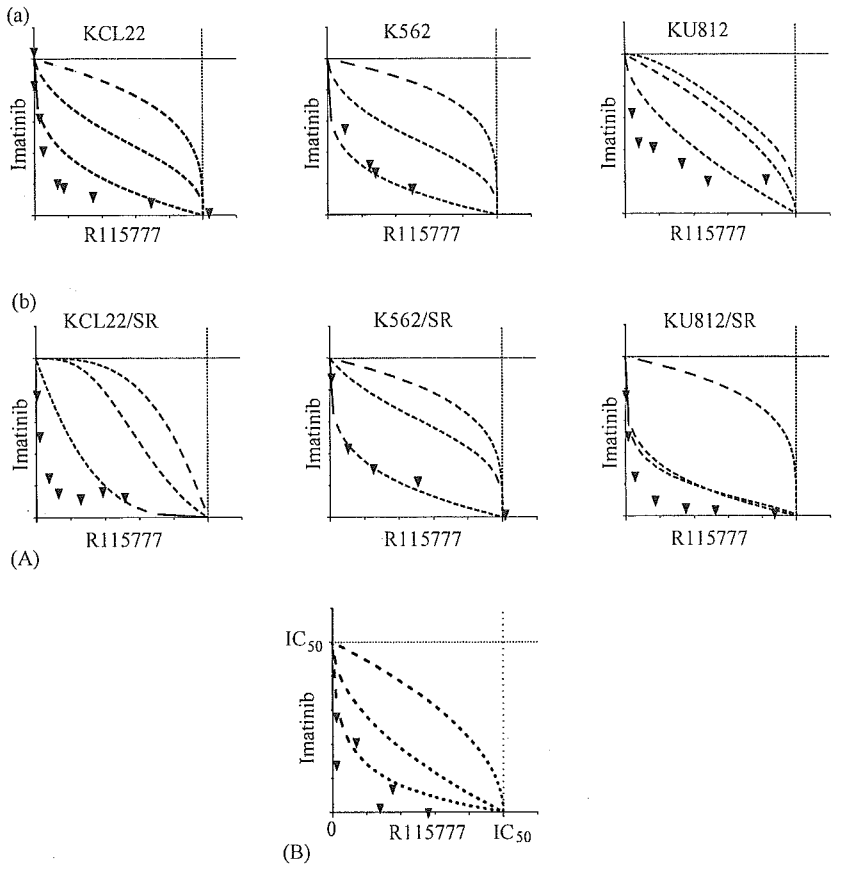

Fig. 1. Effect of combination of R115777 and imatinib on growth inhibition. (A) Steel and Peckham isobologram analyses of the combination of R115777 and imatinib in BCR/ABL-positive cell lines were performed as described in Section 2. Most points are plotted in the area representing synergistic effects in all BCR/ABL-positive parental cell lines (a) and imatinib-resistant cell lines (b). (B) Mononuclear cells from peripheral blood of a patient with imatinib-refractory blast crisis were first seeded at a density of 1×10^5 cells/ml and cultured in RPMI1640 media for 72 h. Steel and Peckham isobologram analysis of the combination of R115777 and imatinib was performed as described in Section 2. Most points are plotted in the area of synergistic effects.

nib-resistant BCR/ABL-positive cells in patients in blast crisis.

3.4. Induction of apoptosis by combination of R115777 and imatinib

To clarify whether the combination of R115777 and imatinib inhibits cell growth due to induction of apoptosis, we examined the levels of cleaved caspase 3, cleaved PARP and the number of annexin-V-positive cells with or without the combination treatment. The combination treatment increased the level of cleaved caspase 3 in all parental and imatinib-resistant cell lines (Fig. 2A). In K562, K562/SR, KU812 and KU812/SR cells, the level of cleaved PARP, which is one of the downstream molecules of caspase 3, was also significantly increased. Consistent with these results, the combination treatment markedly increased the number of annexin-V-positive K562, K562/SR, KU812 and KU812/SR cells, whereas addition of IC_{50} concentrations of imatinib or R115777 alone only slightly increased the number of annexin-V-positive cells (Fig. 2B). In contrast, the level of cleaved PARP was much less increased by the combination treatment in KCL22 and KCL22/SR cells (Fig. 2A). Furthermore, induction of annexin-V-positive cells was much less pronounced in KCL22 and KCL22/SR cells at 72 h (Fig. 2B), 48 h and 96 h (data not shown) after addition of R11577 with imatinib. These results indicate that the combination of R11577 and imatinib induces apoptosis in both imatinib-sensitive and imatinib-resistant cells, but the contribution of apoptosis to the synergistic inhibitory effect on cell growth is relatively low in KCL22 and KCL22/SR cells because of insufficient activation of PARP.

3.5. Effect of the combination of R115777 and imatinib on the cell cycle

Since the combination treatment only slightly increased the number of annexin-V-positive cells in KCL22 and KCL22/SR cells, we hypothesized that the synergistic growth inhibition was mainly caused by induction of cell cycle blockage in these cells. To investigate the function of the G1 checkpoint, we first examined the level of $p27^{KIP1}$. Consistent with our previous findings, $p27^{KIP1}$ expression was up-regulated by treatment with imatinib alone in

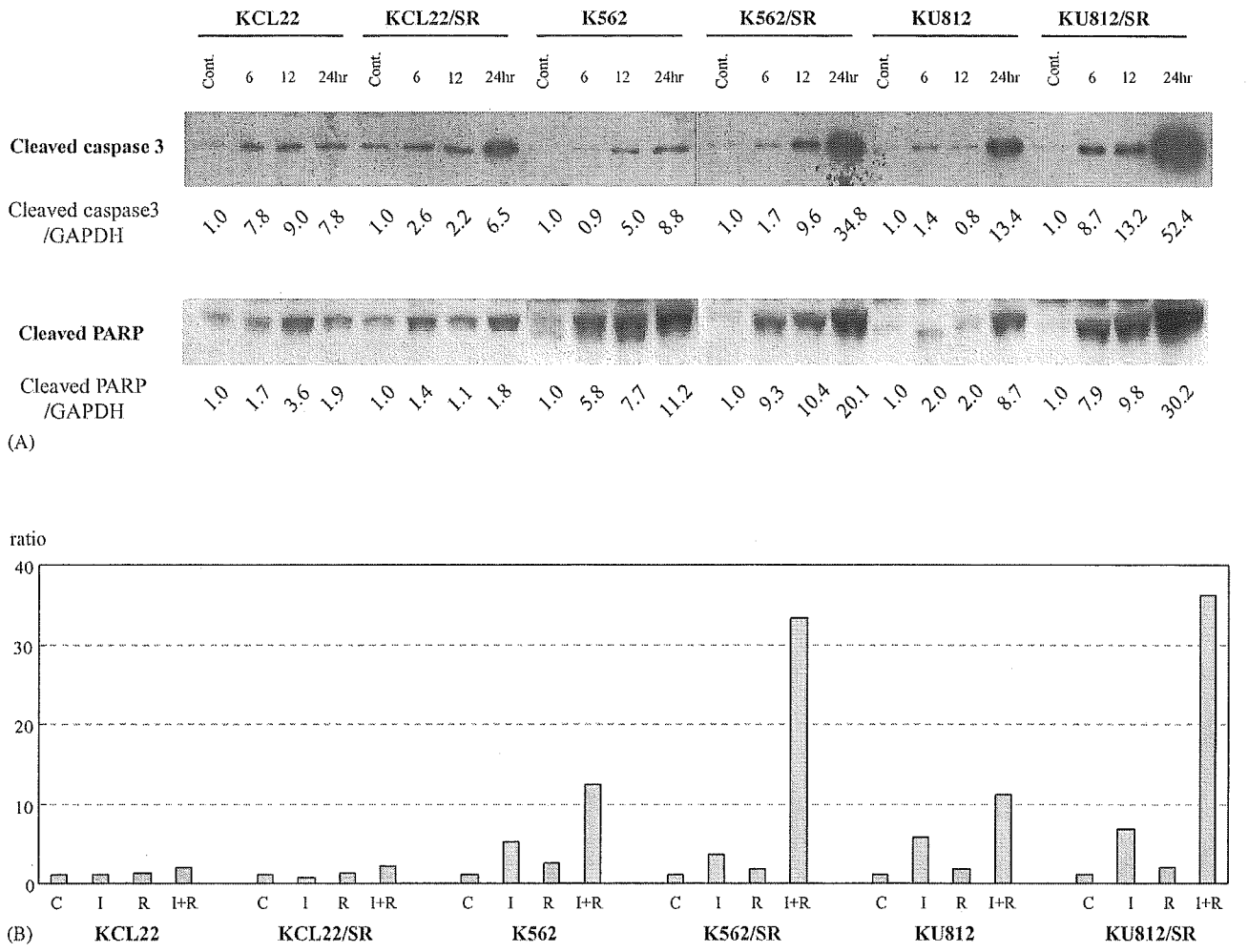

Fig. 2. Induction of apoptosis by a combination of R115777 and imatinib. (A) Cells were cultured in the absence of any reagent for 3 days prior to the treatment and then treated with a combination of IC_{50} concentrations of imatinib and R115777 for 6, 12 and 24 h. Total cell lysates were prepared and subjected to Western blot analysis using anti-cleaved casepase-3 and anti-PARP antibodies. The expression of glyceraldehyde-3-phosphate dehydrogenase (GAPDH) was examined as an internal control. The levels of cleaved caspase 3 and cleaved PARP normalized on the basis of GAPDH levels are shown. (B) Cells were cultured in the absence of any reagent for 3 days prior to treatment and then treated with IC_{50} concentrations of imatinib, R115777 or a combination of imatinib and R115777 for 72 h. The number of annexin-V-positive cells was counted by flow cytometry as described in Section 2.

KCL22 and KCL22/SR cells (Fig. 3A). In these cells, the combination treatment with IC_{50} concentrations of R115777 and imatinib also promoted $p27^{KIP1}$ accumulation and significantly increased the percentage of G0/G1 cells (Fig. 3A and B). To determine whether a higher concentration of imatinib could induce cell cycle progression and thus lead cells to apoptosis, we next examined the effect of combined treatment with 5 μM imatinib and IC_{50} concentration of R115777 on $p27^{KIP1}$ expression and G0/G1 accumulation. The results showed that the combination of the reagents at these concentrations increased $p27^{KIP1}$ level and the percentage of G0/G1 cells to the same level and percentage as those in the case of IC_{50} concentrations of R115777 and imatinib (data not shown). These findings suggest that the combination could not abrogate the imatinib-induced activation of G1 checkpoint and that induction of cell cycle arrest rather than induction of apoptosis was thus the main cause of synergistic growth inhibition in KCL22 and KCL22/SR cells. In contrast, the percentage of G0/G1 cells among K562, KU812, K562/SR or KU812/SR cells was not increased but rather decreased by combination treatment (Fig. 3B). Consistent with these results, the levels of cycline D1 were decreased after combination treatment in K562, KU812, K562/SR and KU812/SR cells (data not shown). The $p27^{KIP1}$ level in KU812/SR cells was slightly increased and maintained for 24 h by treatment with imatinib alone, whereas the level was increased at 6 h but declined afterward in K562, K562/SR and KU812 cells (Fig. 3A). Interestingly, combination treatment with R115777 and imatinib had no inhibitory effect on the imatinib-mediated induction of $p27^{KIP1}$ expression in these cells (Fig. 3A). These results suggest that G0/G1 accumulation was not induced in these cells, unlike in KCL22 and KCL22/SR cells, despite G1 checkpoint activation, probably due to the significant induction of apoptosis after combination treatment.

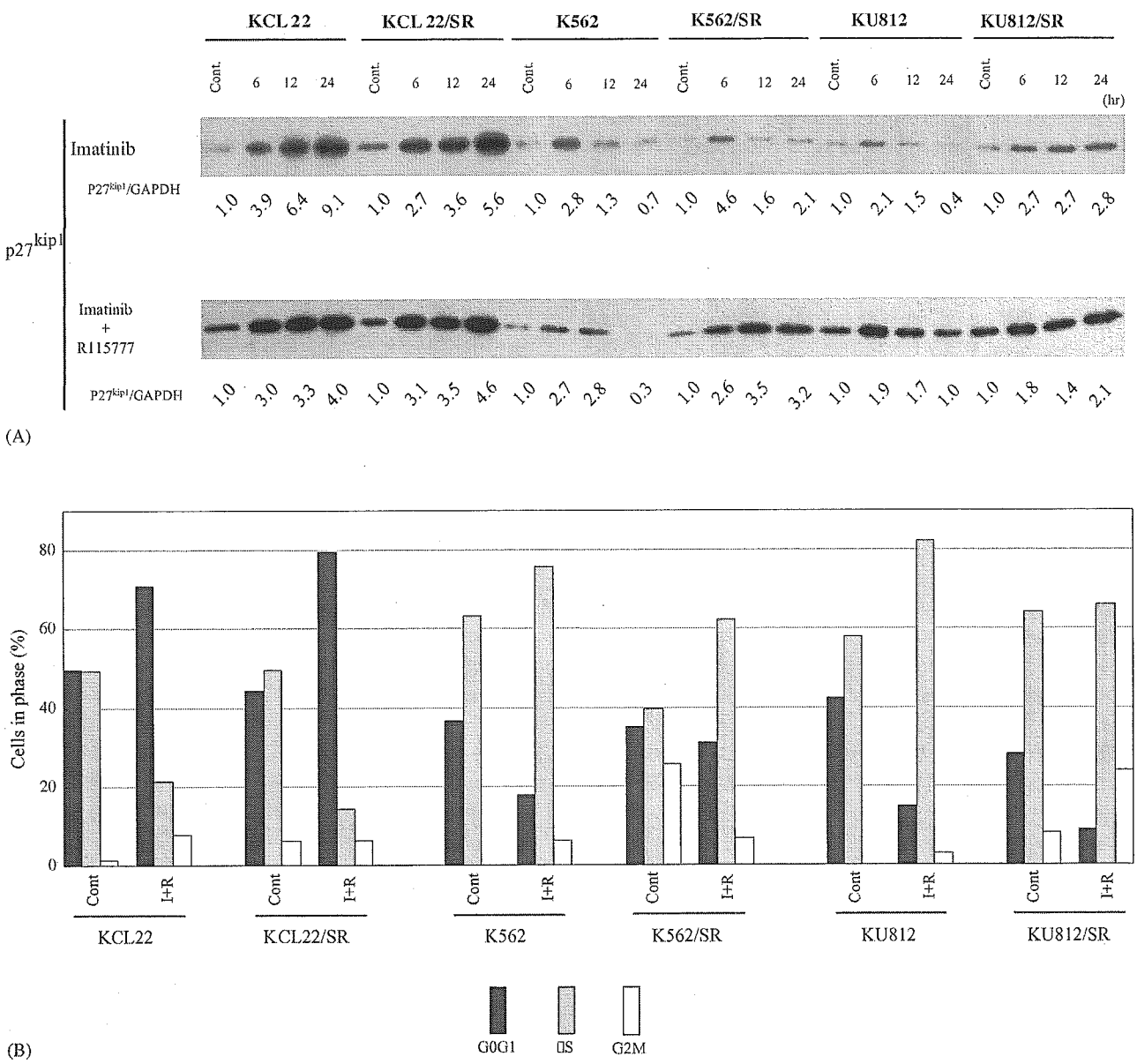

Fig. 3. Effect of combination treatment with R115777 and imatinib on the cell cycle. (A) Changes in $p27^{KIP1}$ protein levels in cells treated with imatinib alone or with a combination of R115777 and imatinib. Cells were cultured in the absence of any reagent for 3 days prior to the treatment and then treated with IC_{50} concentrations of imatinib alone or a combination of IC_{50} concentrations of imatinib and R115777 for 6, 12 and 24 h. Total cell lysates were prepared and subjected to Western blot analysis using anti-$p27^{KIP1}$ antibody. Anti-glyceraldehyde-3-phosphate dehydrogenase (GAPDH) antibody was used as a control for loading (lower panel). (B) Combination treatment of R115777 and imatinib changed the ratios of cell cycle stages. After 24 h of incubation of cells with IC_{50} concentrations of imatinib and R115777, the cells were harvested and incubated with propidium iodide for 30 min and analyzed by flow cytometry with a FACScan/CellFIT system (Becton Dickinson, San Jose, CA).

4. Discussion

Previous studies showed that sustenance of BCR/ABL kinase activity mediated by mechanisms including increased expression of and point mutations in the BCR/ABL gene is a major cause of acquisition of resistance to imatinib [5–14]. In fact, BCR/ABL gene mutations have been found in many clinical imatinib-resistant cases [5–9]. However, there are some cases in which no mutation is found. In the latter cases, deregulation of processes downstream of BCR/ABL kinase may be involved in the resistance to imatinib. Thus, resistance to imatinib can apparently be obtained in both BCR/ABL kinase activity-related and activity-unrelated manners. Imatinib-resistant cell lines examined in the present study exhibited no upregulation of BCR/ABL protein or point mutations in the BCR/ABL gene (data not shown). Moreover, phosphorylation of BCR/ABL was significantly suppressed by imatinib treatment, suggesting that these cells provide a good model of imatinib resistance via a BCR/ABL kinase activity-unrelated mechanism.

FTIs are reagents that may target abnormally activated cellular signaling downstream of BCR/ABL kinase. Previous in vitro studies showed that combinations of FTIs and

imatinib are effective against BCR/ABL-positive cells, but it is unclear whether this effect is additive or synergistic. The present results indicate that combination of R115777 and imatinib synergistically inhibits growth of BCR/ABL-positive cell lines, as indicated by a Steel and Peckham isobologram, which is one of the most reliable methods of analysis for evaluating cell growth inhibition (Fig. 1A). Notably, this synergistic inhibitory effect was also observed in both imatinib-resistant cell lines and leukemia cells from an imatinib-refractory patient (Fig. 1A and B). These results strongly suggest that this combination would have therapeutic value for patients with aggressive BCR/ABL-positive leukemia. It is important to clarify whether the combination treatment is also effective against cells that have resistance-associated mutated BCR/ABL protein, whose kinase activity is not effectively inhibited by imatinib [42]. On the other hand, the contribution of upregulation of P-gp to acquisition of resistance to imatinib is still controversial [43,44]. Fortunately, the effect of the combination treatment may not be influenced by overexpression of P-gp, because the growth of KU812/SR cells (which express P-gp at a level 12.7-fold higher than that in parental KU812 cells) was effectively inhibited by the combination treatment, as was the case with other cell lines.

FTIs were initially developed as inhibitors of posttranslational processing of Ras proteins. However, numerous previous studies suggest that inhibition of the processing of other target proteins such as RhoB, CENP-E and CENP-F is involved in FTI-mediated inhibition of tumor cell proliferation [27,28]. In the present study, R115777 alone had no effect on the levels of phopho-ERK1/2 in any of the BCR/ABL-positive cell lines examined. Taken together with the finding that overexpression of MEK1 (a downstream kinase in the Ras pathway) in KCL22 cells did not restore the cytotoxic effect of the combination treatment (data not shown), this suggests that inhibition of abnormally activated signaling other than Ras-MAPK signaling is involved in synergistic growth inhibition by the combination treatment. We previously found by DNA microarray analyses that RASAP1 and RhoA, which affect or engage in cross talk with cellular signaling, are expressed at higher levels in KCL22/SR cells than in KCL22 cells [36]. It is of interest to clarify whether the effect of the combination treatment is mediated by expression of such molecules.

It has been shown that imatinib induces apoptosis in CML cells [45]. In K562, KU812, K562/SR and KU812/SR cells, R115777 significantly augmented the imatinib-induced increase in the number of annexin-V-positive cells (Fig. 2B). Consistent with these results, the levels of both cleaved caspase 3 and cleaved PARP were increased by the combination treatment. These results suggest that the combination effectively induces apoptosis in these cells. In contrast, the induction of annexin-V-positive cells was extremely low in KCL22 and KCL22/SR cells despite the increase in the level of cleaved caspase 3 by the combination treatment (Fig. 2A and B). One possible explanation for these results is that apoptosis signaling was blocked downstream of caspase 3 in KCL22 and KCL22/SR cells. In fact, the level of cleaved PARP, which is one of the downstream molecules of caspase 3, was much less increased in KCL22 and KCL22/SR cells than in other cell lines (Fig. 2A). Although it is also possible that other unknown mechanisms critically contribute to the blockage of apoptosis, these results suggest that the apoptosis-induction system may break down and that even the combination could not overcome the resistance for the induction of apoptosis in these cells. It is of importance to elucidate the possible unknown mechanisms of apoptosis signaling blockage, and such efforts are now being made in our laboratory.

$p27^{KIP1}$ expression was up-regulated by imatinib alone in all cell lines examined in this study. These results are consistent with our previous findings that imatinib induced cell cycle arrest at the G0/G1 phase, accompanied by up-regulation of $p27^{KIP1}$, in KCL22 cells [46]. Addition of R115777 resulted in no suppression of imatinib-induced up-regulation of $p27^{KIP1}$ expression in all cell lines, suggesting that the combination could not inhibit imatinib-dependent activation of the G1 checkpoint. It is noteworthy that R115777 alone increased the $p27^{KIP1}$ level (in K562, KU812, KCL22 and KCL22/SR cells) or had no effect on the $p27^{KIP1}$ level (in K562/SR and KU812/SR cells) (data not shown). Since FTIs have been shown to induce cell cycle arrest via inhibition of farnesylation of CENP-E protein [47,48], it is possible that CENP-E was a target molecule of R115777 in these cells. Since the apoptosis signal was blocked downstream of caspase 3, the percentage of G0/G1 cells was significantly increased with G1 checkpoint activation after the combination treatment in KCL22 and KCL22/SR cells (Fig. 3A and B). Therefore, it is concluded that cell cycle blockage was mainly involved in the synergistic cell growth inhibition by the combination treatment in KCL22 and KCL22/SR cells. We previously showed that treatment of KCL22 cells with 20 μM imatinib also resulted in G0/G1 accumulation but not in induction of apoptosis [46]. In this study, combined treatment of KCL22 and KCL22/SR cells with R115777 and a higher concentration (5 μM) of imatinib also resulted in G0/G1 accumulation (data not shown). These results suggest that a high concentration of imatinib could not overcome G1 checkpoint activation in these cells.

The other cell lines, K562, KU812, K562/SR and KU812/SR, exhibited different responses. Although the level of $p27^{KIP1}$ was increased by the combined treatment, the percentage of G0/G1 cells was not increased but was rather decreased. The reason for these discrepant phenomena may be the significant induction of apoptosis in these cells. It is likely that apoptosis is induced in the cells before they are led to a G0/G1 state. These results suggest that the induction of apoptosis but not cell cycle blockage plays an important role in the synergistic growth inhibition of K562,

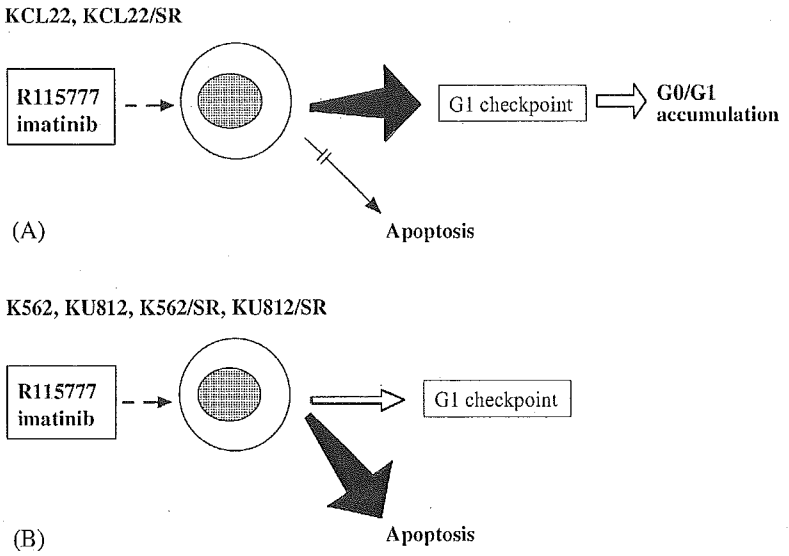

Fig. 4. Hypothetical scheme of the different responses to the combination of R115777 and imatinib in BCR/ABL-positive cells. (A) The combination treatment activates the G1 checkpoint, leading to G0/G1-phase accumulation in KCL22 and KCL22/SR cells, in which apoptosis signaling breaks down. (B) K562, KU812, K562/SR and KU812/SR cells undergo apoptosis with the combination treatment without induction of G0/G1 accumulation.

KU812, K562/SR and KU812/SR cells. A model for the different responses to the combination treatment is presented in Fig. 4. This predicts that the G1 checkpoint remains active but apoptosis signaling breaks down under the condition of combination treatment, leading to G0/G1-phase accumulation in KCL22 and KCL22/SR cells. In contrast, K562, KU812, K562/SR and KU812/SR cells mainly undergo apoptosis by the combination treatment. It is interesting that the imatinib-resistant clone and each corresponding parental cell line showed similar responses to the combination treatment. Therefore, the different pattern of responses might be due to some original cell characteristics, which remain even after acquisition of resistance to imatinib.

The results of this study suggest that the combination treatment of R115777 and imatinib effectively reduce the number of leukemia cells regardless of the sensitivity to imatinib. The finding that the relative importance of the two major mechanisms involved in synergistic inhibition, induction of apoptosis and cell cycle blockage, differed among cell types may have important implications for clinical application of the combination treatment. Since primitive, quiescent BCR/ABL-positive cells may be resistant to imatinib [49], it is likely that KCL22 or KCL22/SR-type leukemia cells, the cell cycles of which are induced to a standstill, may survive after the combination treatment and grow later in the clinical course. Therefore, additional treatment for overriding the G1 checkpoint may be required to eradicate these types of leukemia cells.

Acknowledgments

We are grateful to Drs. Y. Furukawa, T. Kondo, S. Nakano and K. Mitsugi for their helpful discussions. We also thank Ms. E. Yamakawa for her help in preparation of the manuscript. This work was supported by grants-in-aid from the Ministry of Education, Culture, Sports, Science and Technology, Japan.

References

[1] Kantarjian H, Sawyers C, Hochhaus A, Guilhot F, Schiffer C, Gambacorti-Passerini C, et al. Hematologic and cytogenetic responses to imatinib mesylate in chronic myelogenous leukemia. N Engl J Med 2002;346:645–52.
[2] Hughes TP, Kaeda J, Branford S, Rudzki Z, Hochhaus A, Hensley ML, et al. Frequency of major molecular responses to imatinib or interferon alfa plus cytarabine in newly diagnosed chronic myeloid leukemia. N Engl J Med 2003;349:1423–32.
[3] Sawyers CL, Hochhaus A, Feldman E, Goldman JM, Miller CB, Ottmann OG, et al. Imatinib induces hematologic and cytogenetic responses in patients with chronic myelogenous leukemia in myeloid blast crisis: results of a phase II study. Blood 2002;99:3530–9.
[4] Druker BJ, Sawyers CL, Kantarjian H, Resta DJ, Reese SF, Ford JM, et al. Activity of a specific inhibitor of the BCR/ABL tyrosine kinase in the blast crisis of chronic myeloid leukemia and acute lymphoblastic leukemia with the Philadelphia chromosome. N Engl J Med 2001; 344:1038–42.
[5] Shah NP, Nicoll JM, Nagar B, Gorre ME, Paquette RL, Kuriyan J, et al. Multiple BCR-ABL kinase domain mutations confer polyclonal resistance to the tyrosine kinase inhibitor imatinib (STI571) in chronic phase and blast crisis chronic myeloid leukemia. Cancer Cell 2002; 2:117–25.
[6] Gorre ME, Mohammed M, Ellwood K, Hsu N, Paquette R, Rao PN, et al. Clinical resistance to STI571 cancer therapy caused by BCR-ABL gene mutation of amplification. Science 2001;293:876–80.
[7] Branford S, Rudzki Z, Walsh S, Grigg A, Arthur C, Taylor K, et al. High frequency of point mutations clustered within the adenosine triphosphate-binding region of BCR/ABL in patients with chronic myeloid leukemia or Ph-positive acute lymphoblastic leukemia who develop imatinib (STI571) resistance. Blood 2002;99:3472–5.
[8] von Bubnoff N, Schneller F, Peschel C, Duyster J. BCR-ABL gene mutations in relation to clinical resistance of Philadelphia-chromo-

some-positive leukemia to STI571: a prospective study. Lancet 2002;359:487–91.
[9] Ricci C, Scappini B, Divoky V, Gatto S, Onida F, Verstovsek S, et al. Mutation in the ATP-binding pocket of the ABL kinase domain in an STI571-resistant BCR/ABL-positive cell line. Cancer Res 2002; 62:5995–8.
[10] le Coutre P, Tassi E, Varella-Garcia M, Barni R, Mologni L, Cabrita G, et al. Induction of resistance to the Abelson inhibitor STI571 in human leukemic cells through gene amplification. Blood 2000;95:1758–66.
[11] Weisberg E, Griffin JD. Mechanism of resistance to the ABL tyrosine kinase inhibitor STI571 in BCR/ABL-transformed hematopoietic cell lines. Blood 2000;95:3498–505.
[12] Mahon FX, Deininger MW, Schultheis B, Chabrol J, Reiffers J, Goldman JM, et al. Selection and characterization of BCR-ABL positive cell lines with differential sensitivity to the tyrosine kinase inhibitor STI571: diverse mechanisms of resistance. Blood 2000; 96:1070–9.
[13] Gambacorti-Passerini C, Barni R, le Coutre P, Zucchetti M, Cabrita G, Cleris L, et al. Role of α1 acid glycoprotein in the in vivo resistance of human BCR-ABL$^+$ leukemic cells to the Abl inhibitor STI571. J Natl Cancer Inst 2000;92:1641–50.
[14] Tarumoto T, Nagai T, Ohmine K, Miyoshi T, Nakamura M, Kondo T, et al. Ascorbic acid restores the sensitivity to imatinib through suppression of Nrf2-dependent gene expression in a imatinib-resistant cell line, KCL22/SR. Exp Hematol 2004;32:375–81.
[15] Roche-Lestienne C, Soenen-Cornu V, Grardel-Duflos N, Lai JL, Philippe N, Facon T, et al. Several types of mutations of the Abl gene can be found in chronic myeloid leukemia patients resistant to STI571, and they can pre-exist to the onset of treatment. Blood 2002;100:1014–8.
[16] Kreuzer KA, Le Coutre P, Landt O, Na IK, Schwarz M, Schultheis K, et al. Preexistence and evolution of imatinib mesylate-resistant clones in chronic myelogenous leukemia detected by a PNA-based PCR clamping technique. Ann Hematol 2003;82:284–9.
[17] Hofmann WK, Komor M, Wassmann B, Jones LC, Gschaidmeier H, Hoelzer D, et al. Presence of the BCR-ABL mutation Glu255Lys prior to STI571 (imatinib) treatment in patients with Ph+ acute lymphoblastic leukemia. Blood 2003;102:659–61.
[18] La Rosee P, Corbin AS, Stoffregen EP, Deininger MW, Druker BJ. Activity of the Bcr-Abl kinase inhibitor PD180970 against clinically relevant Bcr-Abl isoforms that cause resistance to imatinib mesylate (Gleevec, STI571). Cancer Res 2002;62:7149–53.
[19] Mow BM, Chandra J, Svingen PA, Hallgren CG, Weisberg E, Kottke TJ, et al. Effects of the Bcr/abl kinase inhibitors STI571 and adaphostin (NSC 680410) on chronic myelogenous leukemia cells in vitro. Blood 2002;99:664–71.
[20] Nagar B, Bornmann WG, Pellicena P, Schindler T, Veach DR, Miller WT, et al. Crystal structures of the kinase domain of c-Abl in complex with the small molecule inhibitors PD173955 and imatinib (STI-571). Cancer Res 2002;62:4236–43.
[21] Wisniewski D, Lambek CL, Liu C, Strife A, Veach DR, Nagar B, et al. Characterization of potent inhibitors of the Bcr-Abl and the c-kit receptor tyrosine kinases. Cancer Res 2002;62:4244–55.
[22] Tipping AJ, Melo JV. Imatinib mesylate in combination with other chemotherapeutic drugs: in vitro studies. Semin Hematol 2003; 40(Suppl. 2):83–91.
[23] Druker BJ. Overcoming resistance to imatinib by combining targeted agents. Mol Cancer Ther 2003;2:225–6.
[24] Rowinsky EK, Windle JJ, Von Hoff DD. Ras protein farnesyltransferase: a strategic target for anticancer therapeutic development. J Clin Oncol 1999;17:3631–52.
[25] Gibbs RA. Farnesyltransferase inhibitors: novel anticancer mechanisms and new therapeutic applications. Curr Opin Drug Dis Dev 2000;3:585–96.
[26] Kohl NE, Omer CA, Conner MW, Anthony NJ, Davide JP, deSolms SJ, et al. Inhibition of farnesyltransferase induces regression of mammary and salivary carcinomas in ras transgenic mice. Nat Med 1995;1: 792–7.
[27] Ashar HR, James L, Gray K, Carr D, Black S, Armstrong L, et al. Farnesyl transferase inhibitors block the farnesylation of CENP-E and CENP-F and alter the association of CENP-E with the microtubules. J Biol Chem 2000;275:30451–7.
[28] Lebowitz PF, Prendergast GC. Non-Ras targets of farnesyltransferase inhibitors: focus on Rho. Oncogene 1998;17:1439–45.
[29] Peters DG, Hoover RR, Gerlach MJ, Koh EY, Zhang H, Choe K, et al. Activity of the farnesyl protein transferase inhibitor SCH66336 against BCR/ABL-induced murine leukemia and primary cells from patients with chronic myeloid leukemia. Blood 2001;97:1404–12.
[30] Reichert A, Heisterkamp N, Daley GQ, Groffen J. Treatment of Bcr/Abl-positive acute lymphoblastic leukemia in P190 transgenic mice with the farnesyl transferase inhibitor SCH66336. Blood 2001; 97:1399–403.
[31] Hoover RR, Mahon FX, Melo JV, Daley GQ. Overcoming STI571 resistance with the farnesyl transferase inhibitor SCH66336. Blood 2002;100:1068–71.
[32] Karp JE, Lancet JE, Kaufmann SH, End DW, Wright JJ, Bol K, et al. Clinical and biologic activity of the farnesyltransferase inhibitor R115777 in adults with refractory and relapsed acute leukemias: a phase 1 clinical-laboratory correlative trial. Blood 2001;97:3361–9.
[33] Cortes J, Albitar M, Thomas D, Giles F, Kurzrock R, Thibault A, et al. Efficacy of the farnesyl transferase inhibitor R115777 in chronic myeloid leukemia and other hematologic malignancies. Blood 2003;101:1692–7.
[34] Cortes J, Garcia-Manero G, O'Brien S, Hernandez I, Rackoff W, Faderl S, et al. Phase I study of a imatinib and Tipifarnib (Zarnestra^{TM}, R115777) in patients with chronic myeloid leukemia in chronic phase refractory to imatinib. Blood 2003;102:909a.
[35] Gotlib J, Mauro M, O'Dwyer ME, Fechter L, Dugan K, Kuyl J, et al. Tipifarnib (Zarnestra^{TM}) and imatinib (Gleevec^{TM}) combination therapy in patients with advanced chronic myelogenous leukemia (CML): preliminary results of a phase I study. Blood 2003;102:909a.
[36] Ohmine K, Nagai T, Tarumoto T, Miyoshi T, Muroi K, Mano H, et al. Analysis of gene expression profiles in an imatinib-resistant cell line, KCL22/SR. Stem Cells 2003;21:315–21.
[37] Steel GG, Peckham MJ. Exploitable mechanisms in combined radiotherapy-chemotherapy: the concept of additivity. Int J Radiat Oncol Biol Phys 1979;5:85–91.
[38] Kano Y, Akutsu M, Tsunoda S, Mano H, Sato Y, Honma Y, et al. In vitro cytotoxic effects of a tyrosine kinase inhibitor STI571 in combination with commonly used antileukemic agents. Blood 2001;97: 1999–2007.
[39] Lassar AB, Davis RL, Wright WE, Kadesch T, Murre C, Voronova A, et al. Functional activity of myogenic HLH proteins requires hetero-oligomerization with E12/E47-like proteins in vivo. Cell 1991; 66:305–15.
[40] Nagai T, Harigae H, Ishihara H, Motohashi H, Minegishi N, Tsuchiya S, et al. Transcription factor GATA-2 is expressed in erythroid, early myeloid, and CD34+ human leukemia-derived cell lines. Blood 1994;84:1074–84.
[41] Adjei AA, Davis JN, Erlichman C, Svingen PA, Kaufmann SH. Comparison of potential markers of farnesyltransferase inhibition. Clin Cancer Res 2000;6:2318–25.
[42] Hochhaus A. Cytogenetic and molecular mechanisms of resistance to imatinib. Semin Hematol 2003;40:69–79.
[43] Mahon FX, Belloc F, Lagarde V, Chollet C, Moreau-Gaudry F, Reiffers J, et al. MDR1 gene overexpression confers resistance to imatinib mesylate in leukemia cell line models. Blood 2003; 101:2368–73.
[44] Ferrao PT, Frost MJ, Siah SP, Ashman LK. Overexpression of P-glycoprotein in K562 cells does not confer resistance to the growth inhibitory effects of imatinib (STI571) in vitro. Blood 2003;102: 4499–503.

[45] Jacquel A, Herrant M, Legros L, Belhacene N, Luciano F, Pages G, et al. Imatinib induces mitochondria-dependent apoptosis of the Bcr-Abl-positive K562 cell line and its differentiation towards the erythroid lineage. FASEB J 2003;17:2160–2.
[46] Komatsu N, Watanabe T, Uchida M, Mori M, Kirito K, Kikuchi S, et al. A member of Forkhead transcription factor FKHRL1 is a downstream effector of STI571-induced cell cycle arrest in BCR-ABL-expressing cells. J Biol Chem 2003;278:6411–9.
[47] Ashar HR, James L, Gray K, Carr D, Black S, Armstrong L, et al. Farnesyl transferase inhibitors block the farnesylation of CENP-E and CENP-F and alter the association of CENP-E with the microtubules. J Biol Chem 2000;275:30451–7.
[48] Ashar HR, James L, Gray K, Carr D, McGuirk M, Maxwell E, et al. The farnesyl transferase inhibitor SCH 66336 induces a G(2) → M or G(1) pause in sensitive human tumor cell lines. Exp Cell Res 2001; 262:17–27.
[49] Graham SM, Jorgensen HG, Allan E, Pearson C, Alcorn MJ, Richmond L, et al. Primitive, quiescent, Philadelphia-positive stem cells from patients with chronic myeloid leukemia are insensitive to STI571 in vitro. Blood 2002;99:319–25.

HUMAN CELL(Hum Cell)
Vol. 18 No. 1

Printed in Japan

Original Article Cell Line

Establishment And Characterization Of A Novel Philadelphia-Chromosome Positive Chronic Myeloid Leukemia Cell Line, TCC-S, Expressing P210 And P190 *BCR/ABL* Transcripts But Missing Normal *ABL* Gene

Phan Nguyen Thanh Van[1,3], Phan Thi Xinh[1,3], Yasuhiko KANO[2],
Katsushi TOKUNAGA[3], Yuko SATO[1]

HUMAN CELL(Hum Cell)
Vol. 18 No. 1

Printed in Japan

Original Article Cell Line

Establishment And Characterization Of A Novel Philadelphia-Chromosome Positive Chronic Myeloid Leukemia Cell Line, TCC-S, Expressing P210 And P190 *BCR/ABL* Transcripts But Missing Normal *ABL* Gene

Phan Nguyen Thanh Van[1,3], Phan Thi Xinh[1,3], Yasuhiko KANO[2], Katsushi TOKUNAGA[3], Yuko SATO[1]

<Abstract> A novel Philadelphia-chromosome positive (Ph+) cell line, TCC-S, has been established from a patient with Ph+ chronic myeloid leukemia (CML) in the blastic crisis. TCC-S cells were shown to express both P210 and P190 *BCR/ABL* transcripts by reverse transcriptase-polymerase chain reaction (PCR), although quantitative-PCR revealed that TCC-S cells mainly expressed P210 *BCR/ABL* transcript. Karyotype analysis revealed several triploid clones which constantly harbored two der(9)del(9)(p12)t(9;22)(q34;q11)s and two del(9)(q21)s. The der(9)del(9)(p12)t(9;22)(q34;q11) is rarely found in other CML cell lines. Moreover, to the best of our knowledge, del(9)(q21) resulting in missing of a restrict region including normal *ABL* gene has not been found among CML cell lines previously described. Thus, TCC-S cells with only *BCR/ABL* gene and no normal *ABL* gene may be a useful tool for functional study of *ABL* in Ph+ CML.

Keywords: Philadelphia (Ph) chromosome, chronic myeloid leukemia (CML), P210 *BCR/ABL* transcript, P190 *BCR/ABL* transcript, *ABL*.

[HUMAN CELL 18(1) : 25 - 33, 2005]

Introduction

Chronic myeloid leukemia (CML) is a pluripotent stem cell disease resulting from oncogenic transformation. The hallmark of CML, Philadelphia translocation, t(9;22)(q34;q11) is found in 90 to 95% patients with CML[1),2)]. As the result, a fusion of the *ABL* (Abelson) gene[3)] at chromosome band 9q34 and the *BCR* (breakpoint cluster region) gene[3),4)] at chromosome band 22q11 occurs forming a chimeric *BCR/ABL* gene at 22q11. This chimeric gene is reported to be transcribed to P190[1),5)], P210[1),5)], or P230[5-7)] kDa *BCR/ABL* oncoprotein according to the breakpoint within *BCR*. These *BCR/ABL* oncoproteins show constitutively active tyrosine kinase activity and are implicated in the pathogenesis of CML with diverse actions on hematopoietic cells, including transformation, protection of apoptosis, cell cycle progression, altered cell migration and altered adhesion to the extracellular matrix.

Here, we report establishment of a novel Ph

1: Division of Ultrafine Structure, Department of Pathology, Research Institute of International Medical Center of Japan, Tokyo, Japan.
2: Division of Hematology and Medical Oncology, Tochigi Cancer Center, Tochigi, Japan.
3: Department of Human Genetics, School of International Health, Graduate School of Medicine, The University of Tokyo, Tokyo, Japan.

chromosome positive (Ph+) CML cell line, designated TCC-S, which was derived from a patient with Ph+ CML in the blastic crisis (BC). Karyotype analysis of TCC-S cells revealed several triploid clones which constantly harbored two der(9)del(9)(p12)t(9;22)(q34;q11)s, two del(9)(q21)s and two der(22)t(9;22)(q34;q11)s. More than 40 Ph+ CML cell lines have been established so far, and a missing of whole normal chromosome 9 is occasionally reported among them. However, to the best of our knowledge, this del(9)(q21), resulting in the missing of a restricted region of the long arm of chromosome 9 including normal *ABL* gene at 9q34, has never been found. Thus, TCC-S cells, with only *BCR/ABL* gene and no normal *ABL* gene may provide a useful tool for functional study of normal or altered *ABL* gene in Ph+ CML.

Materials and Methds

Case report

A 46-year-old Japanese man was found to have a leukocytosis at the health examination in August 1988. In June 1989, he took an examination for hematologic malignancies at Utsunomiya Social Insurance Hospital. His bone marrow (BM) was found to be hypercellular with marked increase of myeloid lineage cells without a leukemic hiatus. Cytogenesis study of the BM cells showed 46, XY, t(9;22)(q34;q11) [20/20]. The diagnosis of Ph+ CML in the chronic phase was made. Treatment with 1-2 mg/day carboquone was started. His hematologic findings in December 1989 were as follows: white blood cell (WBC) 10.1×10^6/L (1.0% meta-myelocytes, 74.5% neutrophils, 3.1% eosinophils, 6.1% basophils, 6.1% monocytes and 9.2% lymphocytes), red blood cell $5{,}150\times10^9$/L, hemoglobin 158 g/L, and platelet 595×10^9/L. In September 1991, WBC began to increase with 78% myeloid blasts. The BM aspirate showed hypercellular BM with 73% myeloid blasts which expressed the positivity of CD13 and CD33 and the negativity of peroxidase staining. In October 1991, chromosome study of BM cells showed 46, XY, t(9;22)(q34;q11) as a main clone together with several sub-clones with Ph translocation (Table 1). The diagnosis of the myeloid blastic crisis was made. He was treated with a combined chemotherapy with behenoyl cytarabine (a long-acting depot form of cytarabine)[8], 6-mercaptopurine, daunomycine and prednisone. However, he died from pneumonia on October 31, 1991.

Cell culture

The leukemic cells were obtained from the patient's BM during the blastic crisis in October 1991 with informed content. The cells were cultured in a flask containing RPMI 1640 medium (Sigma Chemical Co., MO, USA) supplemented with 10% heat-inactivated fetal bovine serum (ICN Biochemicals, Irvine, USA), 100 U/mL penicillin and 100 μg/mL streptomycin (Nacalai Tesque, Inc., Kyoto, Japan) (later called as "culture media"), in a humidified atmosphere of 5% CO_2. Half of the culture media was replaced once a week.

Cell morphology

2 to 3 X 10^4 cells were used to prepare slides by using a Shandon Cytospin 2 (Thermo Electron Corporation, Waltham, USA). Cell morphology was observed under a light microscopy after Wright-Giemsa staining.

Immuno-phenotype analysis

Cell surface antigens were analyzed by using a FACsCalibur (BD Bioscience, San Jose, USA). The monoclonal antibodies, CD2, CD3, CD4, CD5, CD7, CD8, CD10, CD13, CD14, CD19, CD20, CD33, CD34, CD56 and HLA-DR, were used with a direct staining technique.

Cytogenetic study

Metaphase slides were prepared with a high-resolution method described elsewhere[9]. In brief, 5 X 10^6 cells were cultured in 10 mL culture media, and were harvested after exposure in 300 μg/mL thymidine (Sigma Chemical Co.) for 16 hours. Then, the cells were exposed to 12.5 μg/mL bromo-deoxyuridine (Wako Pure Chemical Industries, Osaka, Japan) for 5.5 hours, and 0.05 μg/mL demecolchin (Invitrogen Ltd., Carlsbad, USA) for 30 minutes, followed by treatment with 0.05 M KCL for 20 minutes. The cells were fixed with mix of methanol and glacial acetic acid (ratio 3:1). Slides were made with air-dry

method and stained with a dual Q-banding using quinacrine and Hoechst 33258. Twenty-eight metaphases were analyzed by using Macktype v 5.4.2 software (Appied Imaging, Newcastle, UK).

Fluorescence in situ hybridization (FISH) study

To detect a *BCR/ABL* fusion gene, the above-mentioned metaphase slides were used for FISH study, with LSI BCR/ABL ES dual color translocation probe (Vysis Inc., Downers Grove, USA). The probe was hybridized to chromosomes according to the manufacturer's protocol. The metaphase images were captured under a fluororescence microscope, and more than 15 metaphases were analyzed by using Macktype v 5.4.2 software (Appied Imaging).

Detection of P210 and P190 *BCR/ABL* transcripts by reverse transcriptase- polymerase chain reaction (RT-PCR)

Total RNA was extracted by using Sepazol-I reagent (Nacalai Tesque Inc.) according to the manufacturer protocol. All steps were carried out in a laminar hood. RNA pellet was dissolved in 20 μL DEPC water and stored at −80℃ until use. cDNA synthesis was performed in a 30 μL volume containing 1.5 μg RNA, 1.25 μg random hexamers (New England Biolabs,

Table 1: Cytogenetic findings of the patient's bone marrow cells

Date	Stage	Karyotype	No. of metaphases	Total No. of metaphases
Jan. 8, 1990	Dx*	46, XY, t(9;22)(q34;q11)	20	20
April 9, 1990	CP†	46, XY, t(9;22)(q34;q11)	19	20
		46, XY	1	
Dec. 13, 1990	CP†	46, XY, t(9;22)(q34;q11)	20	20
Jan. 16, 1991	CP†	46, XY, t(9;22)(q34;q11)	20	20
Oct. 2, 1991	BC‡	46, XY, t(9;22)(q34;q11)	8	17
		44, XY, -9, t(9;22)(q34;q11), -17, -18, +mar	4	
		45, XY, 7q+, -9, t(9;22)(q34;q11), -17, -18, +2mar	1	
		45, XY, 7q+, -9, t(9;22)(q34;q11), 14q+, -17, -18, +2mar	1	
		44, XY, -9, t(9;22)(q34;q11), +14, -17, -18	1	
		45, XY, 2q-, -9, t(9;22)(q34;q11), +14, -17, -18, +21	1	
		47, XY, -9, -9, -16, -17, -18, 22q-, +22q-, +5mar	1	

*Dx, diagnosis; † CP, chronic phase; ‡ BC, blastic crisis

Hertfordshire, UK), 200 U M-MLV RT, 2mM dNTPs, 0.1mM DTT (Invitrogen Ltd.), 1 μL RNase inhibitor (Promega, Madison, USA) and 6 μL first strand RT buffer, according to the manufacturer's instructions. cDNA product was diluted 3 folds. Two μL diluted cDNA was subsequently mixed with 0.1 μL (0.5 U) AmpliTaq Gold (Applied Biosystems, Foster City, USA),and the following primer set of 1 μL (10 pmol) forward and reverse in a 20 μL reaction mixture. To check quality of RNA and efficiency of cDNA synthesis, the internal control gene, *GAPDH*, was used with a primer set, forward *GAPDH*-F (5'-GCACCGTCAAGGCTGAGAA-3', *GAPDH* exon 4) and reverse *GAPDH*-R (5'-CAACGTAGGTCCACCACTGACACG-3', *GAPDH* exon 8). The primers used in first PCR to detect P210 *BCR/ABL* transcript were forward M-*BCR*-1 (5'-ATCCAAGGCTACGGAGAGGC-3', BCR exon 11), and reverse *ABL*-R1 (5'-ATGGTACCAGGAGTGTTTCTCC-3', *ABL* exon 3). To detect P190 BCR/ABL transcript, forward m-*BCR*-1 (5'-CAACAGTCCTTCGACAGC-3', *BCR* exon 1) and reverse *ABL*-R1 were used. The thermal cycling profile was: 95℃ for 12 minutes, 35 cycles at 95℃ for 30 second, 62℃ for 45 second and a final extension at 72℃ for 10 minutes. The second PCR was performed by using 2 μL of the first PCR product. The primers used for the second PCR to detect P210 *BCR/ABL* transcript were forward M-*BCR*-2 (5'-GGAGCTGCAGATGCTGACCAAC-3', *BCR* exon 13), and reverse *ABL*-R2 (5'-TTCCTTGGAGTTCCAACGAGC-3', *ABL* exon 2). To detect P190 *BCR/ABL* transcript, forward m-*BCR*-2 (5'-CAGTGCCATAAGCGGCACC-3', *BCR* exon 1) and reverse *ABL*-R2 were used. The thermal cycling profile of the second PCR was the same as that of the first PCR. PCR was performed by using a GeneAmp PCR system 9700 (Applied Biosystems). The second PCR product was electrophoresed in a 2% agarose gel containing 0.5μg/mL ethidium bromide in 0.5xTBE. The bands of P210 BCR/ABL and P190 *BCR/ABL* transcripts were visualized under UV light.

Detection of P210 or P190 *BCR/ABL* transcript amount by quantitative-polymerase chain reaction (QT-PCR)

To detect *BCR/ABL* transcript amount, QT-PCR was performed by using an ABI PRISM 7700 sequence detector (Applied Biosystems). The primers and probe used for P210 *BCR/ABL* transcript were forward *BCR*-F (5'-GATGCTGACCAACTCGTGTGTG-3', *BCR* exon 13), reverse *ABL*-R (5'-TGGCCACAAAATCATACAGTGC-3', *ABL* exon 2) and probe *ABL*-P (5'-CCTTCAGCGGCCAGTAGCATCTGACTTT-3', *ABL* exon 2). The primers and probe for P190 *BCR/ABL* transcript were forward bcr-f (5'-CAGTGCCATAAGCGGCACC-3', *BCR* exon 1), reverse abl-r (5'-TTCCTTGGAGTTCCAACGAGC-3', *ABL* exon 2) and probe abl-p (5'-CGCCCTCGTCATCGTTGGGCCAGATCT-3', *ABL* exon 2). The primers and probe for *GAPDH* were forward *GAP*-F (5'-GAAGGTGAAGGTCGGAGTC-3', exon

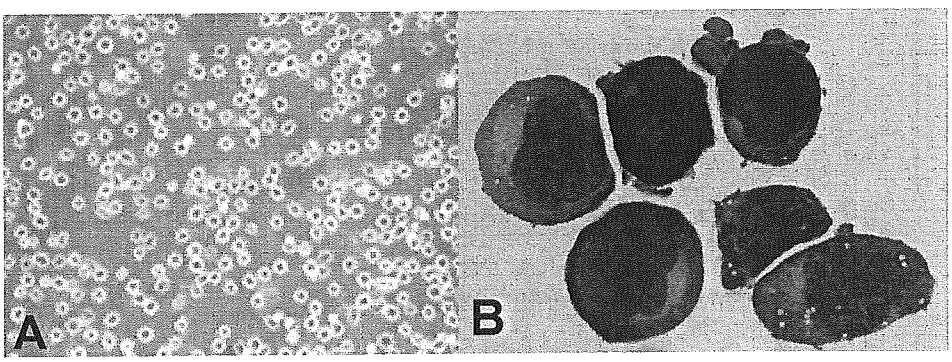

Fig. 1: The morphology of TCC-S cells
A. TCC-S cells looked as round-shaped and non-adherent cells (magnification X 100).
B. In Wright-Giemsa staining, TCC-S cells showed fine chromatin and round nuclei. Cytoplasmic protrusions and small vacuoles were occasionally observed (magnification X 1,000).

2), reverse *GAP*-R (5'-GAAGATGGTGATGGGATTTC-3', exon 4) and probe *GAP*-P (5'-CAAGCTTCCCGTTCTCAGCC-3', exon 4). The result was calculated as a ratio between the amount of *BCR/ABL* and *GAPDH* transcripts.

Results

Establishment and morphology of TCC-S cells

After six weeks' subculture, cells began to grow. In December 1991, a cell line was established and designated TCC-S. TCC-S cells grew well with a doubling time of 27.96 ± 0.97 hours. The cell morphology was observed under a light microscopy after Wright-Giemsa staining by using a cytospin preparation. TCC-S cells had round nuclei with fine chromatin. Cytoplasmic protrusions and small vacuoles were occasionally observed (Figure 1).

Karyotypes and FISH findings

Cytogenetic findings are summarized in Table 2.

Table 2: Cytogenetic findings of the TCC-S cells

Karyotype	No. of metaphases
75, -X, -X, Y, +1, +1, -2, +3, -4, -5, -6, +add(8)(p21), der(9)del(9)(p12)t(9;22)(q34;q11), der(9)del(9)(p12)t(9;22)(q34;q11), del(9)(q21), +del(9)(q21), +add(10)(p14), +11, +11, add(12)(p12), +add(12)(p12), +15, +16, add(17)(p12), +20, -22, der(22)t(9;22)(q34;q11), der(22)t(9;22)(q34;q11), +mar	2
77, XY, -X, +1, add(2)(p23), -3, -4, +6, +7, der(9)del(9)(p12)t(9;22)(q34;q11), der(9)del(9)(p12)t(9;22)(q34;q11), del(9)(q21), +del(9)(q21), +add(10)(p14), +11, +add(12)(p12), +15, +16, add(17)(p12), -18, +19, +20, der(22)t(9;22)(q34;q11), +der(22)t(9;22)(q34;q11)	4
77, -X, -X, Y, +1, add(2)(p23), +3, +6, +7, +add(8)(p21), der(9)del(9)(p12)t(9;22)(q34;q11), der(9)del(9)(p12)t(9;22)(q34;q11), del(9)(q21), +del(9)(q21), -10, +11, +add(11)(p14), +add(12)(p12), +14, add(17)(p12), -18, -18, +19, +20, der(22)t(9;22)(q34;q11), der(22)t(9;22)(q34;q11), +mar	6
76, XY, -X, +1, add(2)(p23), -4, +6, +7, add(8)(p21), der(9)del(9)(p12)t(9;22)(q34;q11), der(9)del(9)(p12)t(9;22)(q34;q11), del(9)(q21), +del(9)(q21), add(10)(p14), +11, +add(12)(p12), +15, add(17)(p12), -18, +19, +21, der(22)t(9;22)(q34;q11), +der(22)t(9;22)(q34;q11)	16
Total No. of metaphases	28

The TCC-S cells showed triploid karyotypes with 67 to 82 chromosomes which constantly harbored two der(9)del(9)(p12)t(9;22)(q34;q11)s and two del(9)(q21)s. A clone with 76 chromosomes was a main one. One of karyotypes with 73 chromosomes is shown in Figure 2A.

FISH study revealed red signal (*ABL* gene) on each of two der(9)s, green signal (*BCR* gene) on one nl(22), and yellow fusion signal (*BCR/ABL* gene) on each of two der(22)s (Figure 2B).

Immuno-phenotype analysis

Expression of surface markers on TCC-S cells and the patient's BM cells is compared in Table 3. The majority of the primary BM cells showed positive for the myeloid markers (CD13 and CD33), CD4 and HLA-DR. Stem cell antigen CD34 was not detected. After establishment of the cell line, expression of HLA-DR was lost, and that of CD33 and CD13 were increased.

Expression of P210 *BCR/ABL* and P190 *BCR/ABL* transcripts

RT-PCR detected both P210 *BCR/ABL* (b3a2 type) and P190 *BCR/ABL* transcripts in TCC-S cells (Figure 3). K562 cells which expressed both transcripts were used as a positive control. QT-PCR detected 209,432 copy/μg of P210 *BCR/ABL* and 1,553 copy/μg of P190 *BCR/ABL* transcript in TCC-S cells.

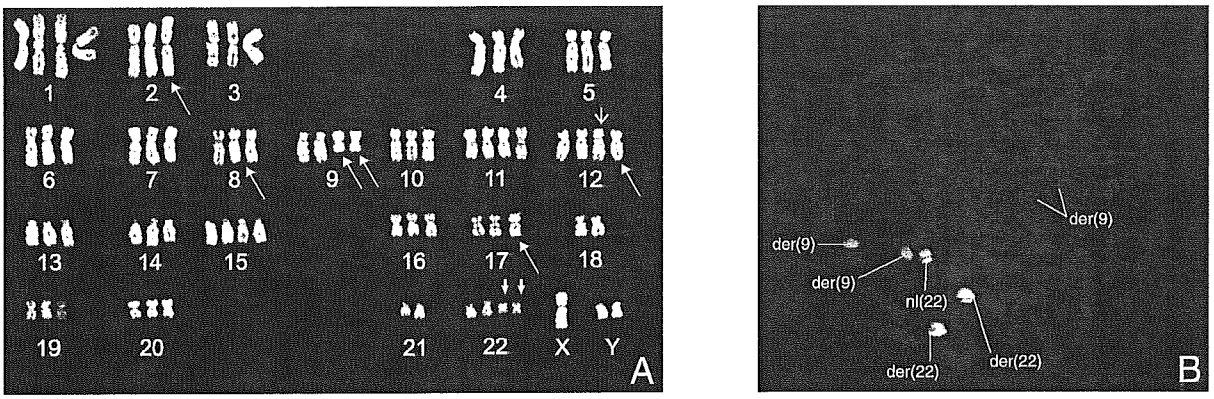

Fig. 2: Karyotype and FISH findings of TCC-S cells
A. One of karyotypes showed 73, XYY, +1, add(2)(p23), add(8)(p21), der(9)del(9)(p12)t(9;22)(q34;q11), der(9)del(9)(p12)t(9;22)(q34;q11), del(9)(q21), +del(9)(q21), +11, add(12)(p11), +add(12)(p12), +15, add(17)(p12), -18, -21, der(22)t(9;22)(q34;q11), +der(22)t(9;22)(q34;q11).
B. The presence of Ph chromosome was confirmed by FISH. FISH revealed red signal (*ABL* gene) on 2 der(9)s, green signal (*BCR* gene) on a nl(22), and yellow fusion signal (*BCR/ABL* gene) on 2 der(22)s.

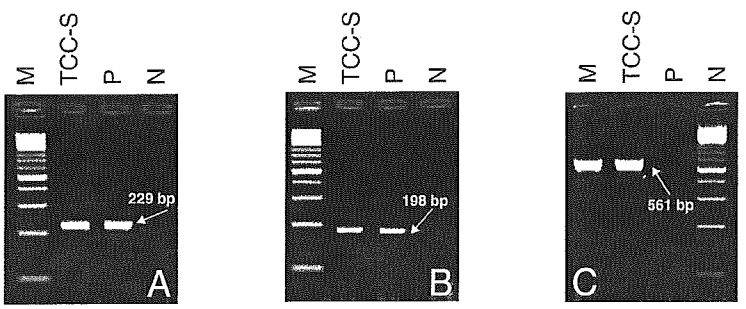

Fig. 3: *BCR/ABL* transcripts in TCC-S cells by RT-PCR
A. P210 *BCR/ABL* (229 bp, b3a2 type) was detected in TCC-S cells.
B. P190 *BCR/ABL* (198 bp, e1a2 type) was also detected in TCC-S cells.
C. *GAPDH* was detected in TCC-S and positive control K562 cells.
M, 100 bp ladder (0.5 μg); P, K562 cells used as a positive control; N, no cells as a negative control